International Journal of Heat and Mass Transfer 65 (2013) 254–264

Contents lists available at SciVerse ScienceDirect

International Journal of Heat and Mass Transfer

journal homepage: www.elsevier.com/locate/ijhmt

Second law analysis for Poiseuille flow of immiscible micropolar fluids in a channel

J.V. Ramana Murthy *, J. Srinivas

Department of Mathematics, National Institute of Technology, Warangal 506 004, AP, India

ARTICLE INFO

Article history:
Received 10 October 2012
Received in revised form 18 April 2013
Accepted 18 May 2013
Available online 2 July 2013

Keywords:
Poiseuille flow
Immiscible fluids
Micropolar fluid
Entropy generation number
Bejan number

ABSTRACT

In this paper, the problem of steady Poiseuille flow of two immiscible incompressible micropolar fluids between two horizontal parallel plates of a channel with constant wall temperatures is studied in terms of entropy generation. The flow is assumed to be governed by Eringen's micropolar fluid flow equations. The flow region is divided into two zones, the flow of the heavier fluid taking place in the lower zone-I. No slip condition is taken on the plates and at the interface continuity of velocity, micro-rotation, temperature, heat flux and shear stresses is imposed. The velocity, micro-rotation and temperature fields are derived analytically. The dimensionless quantities-entropy generation number (Ns), Bejan number (Be) and irreversibility ratio (ϕ) are analytically derived. The effects of material parameters like micropolarity (c_i), couplestress (s_i) on the velocity, micro-rotation and temperature are investigated. The derived equation for the dimensionless entropy generation number is used to interpret the relative importance of frictions to conduction by varying viscous dissipation parameter. The entropy generation near the plates increases more rapidly in fluid I than in fluid II as viscous dissipation effects become more important in zone I. The velocity and temperature profiles are found to be in good agreement with the distributions of the dimensionless entropy generation number (Ns).

1. Introduction

There is a great demand in many industries and projects to thoroughly analyze, improve and design the power systems. In classical methods, the efficiency of the power systems is studied based on first law of thermodynamics. The recent methodologies study the systems based on second law of thermodynamics. The new methodology is called exergy analysis (analysis of available work). In heat transfer process in any system involves exergy losses i.e., destroy the available work due to temperature gradients and fluid frictions. This is due to irreversible work involved in the process. This can be accounted by second law of thermodynamics. Exergy loss is proportional to entropy generation rate. Hence minimization of entropy generation rate indicates optimum exergy or amount of available work. These methods are popularly known as Entropy Generation Minimization (EGM) methods. This was first introduced by Bejan [1,2] and he gave good engineering sense for the study by focusing on irreversibility. This new methodology is based on simultaneous application of first and second law of thermodynamics in analysis and design of the systems. Bejan [1] studied the heat transfer problems in the pipe flow, boundary layer flow past a plate, flow in the entrance region of a rectangular duct using EGM. Bejan [3] demonstrated how the difference between reversible work and work is proportional to entropy generation rate. In the paper he explained how EGM is useful in obtaining optimal allocation of heat transfer area, optimal latent heat storage temperature and optimal sensible heat storage time interval. These methods can be found in detail in the treatises by Bejan [4–7] and Bejan et al. [8].

The flow and heat transfer of immiscible fluids are of special importance in the petroleum extraction and transport problem. The reservoir rock of oil field contains many immiscible fluids in its pores. A portion of the pores contains water and the rest contains oil or gases or both. The immiscible flows in crude oil transport was studied experimentally by Bakhtiyarov et al. [9]. Oscillatory flow and heat transfer in two immiscible viscous fluids was examined analytically by Chamkha [10]. Kamisli et al. [11] explained very nicely the thermodynamic interface conditions involved in a flow of immiscible fluids. They observed that minimum temperature gradient in transverse direction of the flow offers minimum entropy generation near the plates. variation of irreversibility in terms of Bejan number (Be) and energy stream line tracking inside a porous channel are explained in detail by

* Corresponding author. Tel.: +91 870 2462813; mobile: +91 8297831763; fax: +91 8702459547.
E-mail addresses: jvrjosyula@yahoo.co.in, jvr@nitw.ac.in (J.V. Ramana Murthy), j.srinivasnit@gmail.com (J. Srinivas).

0017-9310/$ - see front matter © 2013 Elsevier Ltd. All rights reserved.
http://dx.doi.org/10.1016/j.ijheatmasstransfer.2013.05.048

Nomenclature

Be	Bejan number $\left(=\frac{1}{1+\phi}\right)$
Br	Brinkman number $(=EkPr)$
$\frac{Br}{\Omega}$	viscous dissipation parameter
$c_i=\frac{\kappa_i}{\mu_i}$	material parameter or micropolarity parameter
$\mathcal{C}$	non-dimensional micro-rotation component in z-direction
d_{ij}	components of the strain
D	deformation tensor
E	specific internal energy
Ek	Eckert number
$\bar{f}$	body forces per unit mass
2h	height of the free channel
$\bar{\mathbf{h}}$	heat flux
j	gyration coefficient
k_1, k_2	thermal conductivity of the fluid in zones-I, II
$\bar{l}$	body couple per unit mass
m_{ij}	couple stress tensor
n_β	ratio of couple stress viscosity coefficients $\left(=\frac{\beta_2}{\beta_1}\right)$
n_k	ratio of thermal conductivities $\left(=\frac{k_2}{k_1}\right)$
n_μ	ratio of viscosities $\left(=\frac{\mu_2}{\mu_1}\right)$
n_ρ	ratio of densities $\left(=\frac{\rho_2}{\rho_1}\right)$
Nf_i	entropy generation due to viscous dissipation
Ns_i	dimensionless total entropy generation number
Ny_i	entropy generation due to transverse conduction
Nu	Nusselt number
P	pressure
Pr	Prandtl number
$\bar{q}$	velocity vector
Re	Reynolds number
s_1,s_2	couple stress parameters
$(S_i)_G$	entropy generation rate
$(S_i)_{G,C}$	characteristic entropy transfer rate
t_{ij}	stress tensor
T_1, T_2	non-dimensional temperatures of the plates
u	non-dimensional velocity in X-direction
x, y	non-dimensional space coordinates
X, Y	space co-ordinates

Greek symbols

α, β, γ	gyration viscosity coefficients
δ_{ij}	kronecker delta
δ_1	couple stress parameter $\left(=\frac{\beta_1}{\mu_1 h^2}\right)$
ϵ_{ijk}	Levi–Civita symbol or permutation symbol
κ_1, κ_2	micro-rotation viscosity coefficients
μ_1, μ_2	viscosity coefficients
$\bar{\nu}$	micro-rotation vector
$\mathbf{\Omega}$	dimensionless temperature difference $\left(=\frac{\Delta T}{T_o}\right)$
$\mathbf{\Phi}$	dissipation function
ϕ	irreversibility distribution ratio $\left(=\frac{Nf}{Ny}\right)$
ρ	density
θ	non-dimensional temperature

Subscripts

1	fluid in zone I
2	fluid in zone II

Shohel Mahmud et al. [12]. The effect of geometric parameters to find optimum shape of the ducts by using second law analysis is studied by Sahin [13–15] and Hakan [16].

This paper aims at second law analysis for the flows of two immiscible micropolar fluids in a parallel plate channel. Micropolar fluids exhibit couple stresses and the particles of the fluid have independent rotation vector in addition to velocity vector. This theory of micropolar fluids was proposed by Eringen [17,18]. For experimental determination of parameters of micropolar fluids one can refer Migun et al. [19] and Kolpashchikov et al. [20]. An account of the earlier developments in polar fluid theory can be found in the book by V.K.Stokes [21]. Some basic viscous flows in micropolar fluids was discussed by Ariman et al. [22] and the existing state of art can be seen in the excellent treatise of Lukaszewicz [23]. Jerome et al. [24] gave molecular interpretation for the Poiseuille flow of a micropolar fluid.

The problem of simultaneous flow of immiscible fluids in channels is of importance in industrial processes such as transportation of two or more fluids in the same pipe or channel. So there has been widespread interest in the study of flow through channel and tubes in the recent years. In many of the areas fluid flow, flow of immiscible liquids or multi-phase fluids occur. For example blood flow in arteries has been studied by many researchers considering blood as two phase flow [25]. In view of these, several investigations on multiphase flows are reported by various researchers. Bird et al. [26] found an exact solution for the laminar flow of two immiscible fluids between two parallel plates. Kapur et al. [27] have studied the flow of two immiscible incompressible viscous fluids between two parallel plates. Bhattacharya [28] discussed the flow of immiscible fluids between rigid plates with a time dependent pressure gradient. Mass transfer into a laminar fluid stream from the moving interface of two immiscible fluids between parallel plates was discussed by Hikita et al.[29]. Jie Li et al. [30] have discussed numerical study of flows of two immiscible liquids at low Reynolds number. Chamka et al. [31] discussed flow of two immiscible fluids in a porous and non-porous channel. Malashetty et al. [32] have discussed the convective magnetohydrodynamic two fluid flow and heat transfer in an inclined channel. Umavathi et al. [33] studied unsteady two-fluid flow and heat transfer in a horizontal channel. Prathap Kumar et al. [34] analytically examined fully-developed free-convective flow of micropolar and viscous fluids in a vertical channel. Dragis Nikodijevic et al. [35] have studied MHD Couette two-fluid flow and heat transfer in presence of uniform inclined magnetic field. The heat transfer of two immiscible fluids in the presence of uniform inclined magnetic field was discussed by Nikodijevic et al. [36]. Szeri et al. [37] discussed the flow of a non-Newtonian fluid between heated parallel plates. Nield et al. [38] discussed thermally developing forced convection in a porous medium between two parallel plates with walls maintained at uniform temperature.

The present study is taken up in view of realistic situations cited in [9,25] and growing importance of study of entropy generation methods (EGM). Many researchers considered the immiscible flow of viscous fluids. But very few [33] have taken up the study of micropolar fluids. Since micropolar fluids represent the more general and realistic study of properties of crude oils, blood, etc. Here we are considering the flow of immiscible micropolar fluids between the parallel plates.

2. Fomulation of the problem

The physical model of the flow shown in Fig. 1, consists of two parallel plates extending in the X-direction. The height between the plates is 2h. The plates are maintained at constant temperatures. The width of the plates is much greater than the distance be-

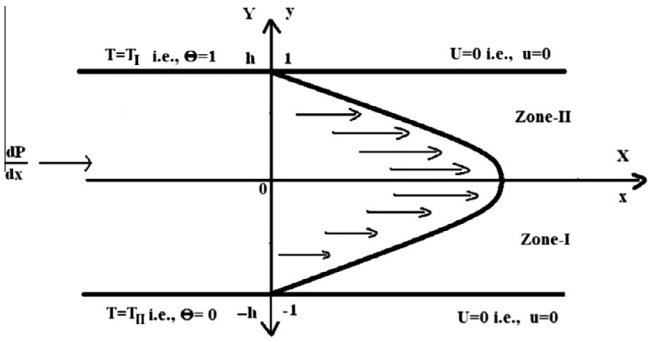

Fig. 1. Schematic of the investigated problem.

tween them. X and Y are the axial and transverse coordinates respectively with the origin at the centre of the channel. A constant pressure gradient acts at the mouth of the channel. The lower fluid (viscosity μ_1, micropolarity κ_1, density ρ_1 and thermal conductivity k_1) occupies the region $-h < Y < 0$ comprising the lower half of the channel and this region is named as zone I. The upper fluid (viscosity μ_2, micropolarity κ_2, density ρ_2 ($<\rho_1$) and thermal conductivity k_2) is assumed to occupy the upper half of the channel (i.e., $0 < Y < h$), and this region is called zone II. In the present case, fluid in zone I is denser than the fluid in zone II. The two walls of the channel are held at different temperatures T_I and T_{II} with $T_I < T_{II}$. The equations for the flow in zone I and II (i.e., $-h < Y < h$) are assumed to be governed by incompressible micropolar fluid flow equations of Eringen [17,18] and energy equation

$$\frac{\partial \rho}{\partial t} + \nabla \cdot (\rho \bar{q}) = 0 \tag{1}$$

$$\rho \frac{d\bar{q}}{dt} = \rho \bar{f} - \nabla P + \kappa \nabla \times \bar{v} - (\mu + \kappa)\nabla \times \nabla \times \bar{q} + (\lambda + 2\mu + \kappa)\nabla(\nabla \cdot \bar{q}) \tag{2}$$

$$\rho j \frac{d\bar{v}}{dt} = \rho \bar{\ell} - 2\kappa \bar{v} + \kappa \nabla \times \bar{q} - \gamma \nabla \times \nabla \times \bar{v} + (\alpha + \beta + \gamma)\nabla(\nabla \cdot \bar{v}) \tag{3}$$

$$\rho \frac{dE}{dt} = -P(\nabla \cdot \bar{q}) + \rho \Phi - (\nabla \cdot \bar{\mathbf{h}}) \tag{4}$$

where

$$\rho\Phi = \lambda(\nabla \cdot \bar{q})^2 + 2\mu(D : D) + 4\kappa\left(\frac{1}{2}\nabla \times \bar{q} - \bar{v}\right)^2 + \alpha(\nabla \cdot \bar{v})^2 + \gamma(\nabla \bar{v} : \nabla \bar{v}) + \beta(\nabla \bar{v} : (\nabla \bar{v})^T)$$

The Eqs. (1)–(4) represent conservation of mass, balance of linear momentum, angular momentum and energy equation respectively. The scalar quantities ρ and j are, respectively, the density and gyration coefficient and are assumed to be constants. The vectors $\bar{q}$, $\bar{v}$, $\bar{f}$ and $\bar{\ell}$ are the velocity, micro-rotation, body force per unit mass and body couple per unit mass, respectively. P is the fluid pressure at any point. The material constants (λ, μ, κ) are viscosity coefficients and (α, β, γ) are gyro-viscosity coefficients. These confirm to the inequalities, $\kappa \geqslant 0$; $2\mu + \kappa \geqslant 0$; $3\lambda + 2\mu + \kappa \geqslant 0$, $\gamma \geqslant 0$; $|\beta| \leqslant \gamma$; $3\alpha + \beta + \gamma \geqslant 0$. And in the energy equation Φ is the dissipation function of mechanical energy per unit mass, D denotes the deformation tensor i.e., $D = \frac{1}{2}(\bar{q}_{i,j} + \bar{q}_{j,i})$, E is the specific internal energy and $\bar{\mathbf{h}} = -k\nabla T$ is the heat flux, where k is the thermal conductivity.

We remark that for $\kappa = \alpha = \beta = \gamma = 0$, and vanishing $\bar{l}$ and $\bar{f}$, micro-rotation $\bar{v}$ becomes zero, and Eq. (2) reduces to the classical Navier–Stokes equations. Also we note that for $\kappa = 0$, the velocity $\bar{q}$ and the micro-rotation $\bar{v}$ are not coupled and the micro-rotations do not effect the velocity field.

The stress tensor t_{ij} and the couple stress tensor m_{ij} are given by

$$t_{ij} = (-P + \lambda div(\bar{q}))\delta_{ij} + (2\mu + \kappa)d_{ij} + \kappa\epsilon_{ijm}(\omega_m - v_m) \tag{5}$$

$$m_{ij} = \alpha v_{r,r}\delta_{ij} + \beta v_{i,j} + \gamma v_{j,i} \tag{6}$$

where v_i and ω_i are the components of the micro-rotation vector and the vorticity vector respectively, d_{ij} are the components of rate of shear strain, δ_{ij} is the Kronecker symbol, ϵ_{ijm} is the Levi–Civita symbol given by 1 if i, j, m are cyclic, -1 if i, j, m are acyclic and 0 if any two of i, j, m are equal and comma denotes covariant differentiation.

To develop the governing equations for the considered model, the following assumptions are made:

(i) The flow is assumed to be one-dimensional and steady.
(ii) The fluids are assumed to be incompressible.
(iii) The gravity effect is negligible.

We assume that the velocity of the fluid to be $\bar{q} = (U(Y), 0, 0)$ and micro-rotation vector as $\bar{v} = (0, 0, C(Y))$.

We introduce the non-dimensional variables:

$$x = \frac{X}{h}, \quad y = \frac{Y}{h}, \quad u = \frac{U}{U_o}, \quad p = \frac{P}{\rho_1 U_o^2}, \quad C = \frac{CU_o}{h}$$

where U_o is the maximum velocity of the fluid in the channel. Equation of continuity (1) is satisfied identically for the assumed form of velocity and neglecting body forces and body couples from Eqs. (2) and (3), we get the following sets of non-dimensional form of governing equations and boundary conditions corresponding to the flow in two zones.

3. Governing equations

We take velocity and micro-rotation as

$$u(y) = \begin{cases} u_1(y) & -1 \leqslant y \leqslant 0 \\ u_2(y) & 0 \leqslant y \leqslant 1 \end{cases} \text{ and } \mathcal{C}(y) = \begin{cases} \mathcal{C}_1(y) & -1 \leqslant y \leqslant 0 \\ \mathcal{C}_2(y) & 0 \leqslant y \leqslant 1 \end{cases}$$

Zone-I: $(-1 \leqslant y \leqslant 0)$

The governing equations in the zone I can be written as:

$$\frac{d^2u_1}{dy^2} + \left(\frac{c_1}{1+c_1}\right)\frac{d\mathcal{C}_1}{dy} = \left(\frac{1}{1+c_1}\right)Re\frac{dp}{dx} \tag{7}$$

$$\frac{d^2\mathcal{C}_1}{dy^2} - s_1\frac{du_1}{dy} - 2s_1\mathcal{C}_1 = 0 \tag{8}$$

Zone-II: $(0 \leqslant y \leqslant 1)$

The governing equations in the zone II can be written as:

$$\frac{d^2u_2}{dy^2} + \left(\frac{c_2}{1+c_2}\right)\frac{d\mathcal{C}_2}{dy} = \left(\frac{1}{1+c_2}\right)\frac{n_\rho}{n_\mu}Re\frac{dp}{dx} \tag{9}$$

$$\frac{d^2\mathcal{C}_2}{dy^2} - s_2\frac{du_2}{dy} - 2s_2\mathcal{C}_2 = 0 \tag{10}$$

where $Re = \frac{\rho_1 U_o h}{\mu_1}$, $c_i = \frac{\kappa_i}{\mu_i}$, $s_i = \frac{\kappa_i h^2}{\gamma_i}$ and $n_\mu = \frac{\mu_2}{\mu_1}$, ($i$ = 1,2).

4. Boundary and interface conditions

A characteristic feature of the two-layer flow problem is the coupling across liquid/liquid interfaces.The liquid layers are mechanically coupled via transfer of momentum across the interfaces. Transfer of momentum results from the continuity of inter-

face tangential velocity and from a stress balance across the interface. The above Eqs. (7)–(10) are solved using the following boundary conditions.

4.1. Poiseuille flow: (flow due to applied pressure gradient)

The plates are kept fixed and the flow is maintained by constant pressure gradient. Hence $\frac{dp}{dx} = B$ = constant. The boundary conditions are given as: At the lower plate boundary velocity and micro-rotation vanish due to no slip and hyper-stick conditions:

$$u_1 = 0 \text{ and } \mathcal{C}_1 = 0 \quad \text{at } y = -1 \tag{11}$$

At the fluid interface velocity, micro-rotation, shear stress and couple stress are continuous:

$$u_1 = u_2,\ \mathcal{C}_1 = \mathcal{C}_2,\ \tau_{xy}|_1 = \tau_{xy}|_2 \text{ and } m_{xy}|_1 = m_{xy}|_2 \quad \text{at } y = 0 \tag{12}$$

At the upper plate boundary the velocity and micro-rotation vanish due to no slip and hyper-stick conditions:

$$u_2 = 0 \quad \textit{and} \quad \mathcal{C}_2 = 0 \quad \textit{at} \quad y = 1 \tag{13}$$

Shear stress and couple stresses are taken from Eqs. (5) and (6)

4.2. Note on hyper stick condition

The hyper-stick condition is taken at the boundary as: The micro-rotation vector on the boundary = angular velocity of the fluid on the boundary, i.e., $C_{wall} = \frac{1}{2}(\nabla \times \overline{Q}_{wall})$. A more general condition is taken as $\mathcal{C}_{wall} = \frac{n}{2}(\nabla \times \bar{q}_{wall})$ where $0 \leqslant n \leqslant 1$ (Refer Lukaszewicz [23], p. 31). This value of n indicates the concentration of micropolarity or interaction of fluid particles with the boundary. The case $n = 0$ indicates $\mathcal{C} = 0$ at the plates. It represents flow of concentrated particles in which the microelements closed to the wall surface are unable to rotate (Jena [39]). This case is also known as strong concentration of microelements. The case corresponding to $n = 0.5$ results in the vanishing of antisymmetric part of stress tensor and represents weak concentrations of microelements. The particle spin is equal to fluid vorticity at the boundary for the fine particle suspensions. The case corresponding to n = 1 is representative of turbulent boundary layer flows (Peddieson [40]). Here we are considering the case $n = 0$. Authors Rees et al. [41] and Bhattacharyya et al. [42] have used this more general condition.

4.3. Shear stress

The dimensionless non-zero shear stress at fluid interface is given by

$$\tau_{xy} = \left[\frac{\partial u_i}{\partial y} + 2\left(\frac{c_i}{1+c_i}\right)\mathcal{C}_i\right]_{y=0}, i = 1, 2 \tag{14}$$

The dimensionless shear stress at the lower and upper boundaries are given by

$$\tau_{xy} = \left[\frac{\partial u_1}{\partial y}\right]_{y=-1}, \quad \tau_{xy} = \left[\frac{\partial u_2}{\partial y}\right]_{y=1} \tag{15}$$

4.4. Couple stress

The dimensionless non-zero couple stress at the interface is given by

$$m_{xy}|_1 = \frac{\partial \mathcal{C}_1}{\partial y}, \quad m_{xy}|_2 = n_\beta \frac{\partial \mathcal{C}_2}{\partial y} \quad \textit{where} \quad n_\beta = \frac{\beta_2}{\beta_1} \quad \textit{at} \quad y = 0 \tag{16}$$

The elaborated expressions are not reported for brevity.

5. Solution of the problem

5.1. Velocity and micro-rotation distributions

Zone-I: $(-1 \leqslant y \leqslant 0)$

Eliminating $\mathcal{C}_1$ from (7), (8) we have

$$\frac{d^4u_1}{dy^4} - s_1\left(\frac{2+c_1}{1+c_1}\right)\frac{d^2u_1}{dy^2} = -\frac{2s_1}{(1+c_1)}Re\ B \tag{17}$$

Substituting $\frac{d\mathcal{C}_1}{dy}$ from (7) in (8) we have

$$\mathcal{C}_1(y) = -\frac{1}{2}\frac{du_1}{dy} - \frac{(1+c_1)}{2c_1s_1}\frac{d^3u_1}{dy^3} \tag{18}$$

Solving (17) we get,

$$u_1(y) = c_{11} + c_{12}y + c_{13}\cosh\alpha_1 y + c_{14}\sinh\alpha_1 y + \frac{ReB}{(2+c_1)}y^2 \tag{19}$$

and substituting $u_1(y)$ in (18) we have

$$\mathcal{C}_1(y) = -\frac{c_{12}}{2} - \alpha_1\left(\frac{1+c_1}{c_1}\right)(c_{13}\sinh\alpha_1 y + c_{14}\cosh\alpha_1 y) - \frac{ReB}{(2+c_1)}y \tag{20}$$

Zone-II: $(0 \leqslant y \leqslant 1)$

Eliminating $\mathcal{C}_2$ from (9), (10) we have

$$\frac{d^4u_2}{dy^4} - s_2\left(\frac{2+c_2}{1+c_2}\right)\frac{d^2u_2}{dy^2} = -\frac{2s_2}{(1+c_2)}\frac{n_\rho}{n_\mu}Re\ B \tag{21}$$

Substituting $\frac{d\mathcal{C}_2}{dy}$ from (9) in (10) we have

$$\mathcal{C}_2(y) = -\frac{1}{2}\frac{du_2}{dy} - \frac{(1+c_2)}{2c_2s_2}\frac{d^3u_2}{dy^3} \tag{22}$$

Solving (21) we get,

$$u_2(y) = c_{21} + c_{22}y + c_{23}\cosh\alpha_2 y + c_{24}\sinh\alpha_2 y + \frac{1}{(1+c_2)} \times \frac{n_\rho}{n_\mu}Re\ B\ y^2 \tag{23}$$

and substituting $u_2(y)$ in (22), we have

$$\mathcal{C}_2(y) = -\frac{c_{22}}{2} - \alpha_2\left(\frac{1+c_2}{c_2}\right)(c_{23}\sinh\alpha_2 y + c_{24}\cosh\alpha_2 y) - \frac{1}{(1+c_2)}\frac{n_\rho}{n_\mu}ReBy \tag{24}$$

where $\alpha_1^2 = s_1\left(\frac{2+c_1}{1+c_1}\right), \alpha_2^2 = s_2\left(\frac{2+c_2}{1+c_2}\right)$.

The solutions $u_1(y)$, $\mathcal{C}_1(y)$ and $u_2(y)$, $\mathcal{C}_2(y)$ involve 8 constants $c_{11}, c_{12}, c_{13}, c_{14}, c_{21}, c_{22}, c_{23}$ and c_{24}. These constants are found from the 8 boundary conditions given in (11)–(13) and they are solved using Mathematica. As the expressions are cumbersome, they are not presented here.

5.2. Volumetric flow rate

The non-dimensional volumetric flow rate of the channel is given by $q = q_1 + q_2$ where

$$q_1 = \int_{-1}^{0} u(y)dy = \frac{c_{14}}{\alpha_1} - c_{11} + \frac{c_{12}}{2} - \frac{c_{13}}{\alpha_1}\sinh\alpha_1 + \frac{c_{14}}{\alpha_1}\cosh\alpha_1 - \frac{ReB}{3(2+c_1)} \tag{25}$$

$$q_2 = \int_{0}^{1} u(y)dy = -\frac{c_{24}}{\alpha_2} + c_{21} + \frac{c_{22}}{2} + \frac{c_{23}}{\alpha_2}\sinh\alpha_2 + \frac{c_{24}}{\alpha_2}\cosh\alpha_2 + \frac{ReB}{3(2+c_2)}\frac{n_\rho}{n_\mu} \tag{26}$$

5.3. Temperature distribution

Once the velocity and micro-rotation distributions are known, the temperature distributions for the two zones are determined by solving the energy equation (4) in the respective zones, subject to the appropriate boundary and interface conditions. Thermal coupling is achieved through continuity of temperature at the interface and the balance of heat flux across the interface. In the present problem, it is assumed that the two walls are maintained at constant temperatures T_I and T_{II} ($T_I < T_{II}$).

We take temperature $T(Y)$ as,

$$T(Y) = \begin{cases} T_1(Y) & -h \leqslant Y \leqslant 0 \\ T_2(Y) & 0 \leqslant Y \leqslant h \end{cases}$$

The governing equation for the temperature T_1 of the conducting fluid in zone I is then given by

$$k_1 \frac{d^2T_1}{dY^2} = -\left[\mu_1\left(\frac{dU_1}{dY}\right)^2 + \kappa_1\left(\frac{dU_1}{dY} + 2C_1\right)^2 + \beta_1\left(\frac{dC_1}{dY}\right)^2\right] \tag{27}$$

The governing equation for the temperature T_2 of the conducting fluid in zone II is then given by

$$k_2 \frac{d^2T_2}{dY^2} = -\left[\mu_2\left(\frac{dU_2}{dY}\right)^2 + \kappa_2\left(\frac{dU_2}{dY} + 2C_2\right)^2 + \beta_2\left(\frac{dC_2}{dY}\right)^2\right] \tag{28}$$

In order to non-dimensionalize the above equations, the following transformation is used in addition to those already introduced in above: $\theta = \frac{T-T_I}{T_{II}-T_I}$.

The Eqs. (27) and (28) are then reduced to the following form:

$$\frac{d^2\theta_1}{dy^2} = -Br\left[\left(\frac{du_1}{dy}\right)^2 + c_1\left(\frac{du_1}{dy} + 2\mathcal{C}_1\right)^2 + \delta_1\left(\frac{d\mathcal{C}_1}{dy}\right)^2\right] \tag{29}$$

$$\frac{d^2\theta_2}{dy^2} = -\frac{Br}{n_k}\left[n_\mu\left(\left(\frac{du_2}{dy}\right)^2 + c_2\left(\frac{du_2}{dy} + 2\mathcal{C}_2\right)^2\right) + n_\beta\delta_1\left(\frac{d\mathcal{C}_2}{dy}\right)^2\right] \tag{30}$$

where $Br = Ek\,Pr$ (Brinkman number), $Ek = \frac{U_o^2}{c_{p_1}(T_2-T_1)}$ (Eckert number), $Pr = \frac{\mu_1 c_{p_1}}{k_1}$ (Prandtl number), $n_k = \frac{k_2}{k_1}$, $n_\beta = \frac{\beta_2}{\beta_1}$ (Ratio of couple stress coefficients) and $\delta_1 = \frac{\beta_1}{\mu_1 h^2}$ (couple stress parameter).

In the non-dimensional form, the boundary conditions for temperature and heat flux at the walls and interface become:

(i) at the lower and upper plate boundaries the temperatures are respectively,

$$\theta_1 = 0 \quad at \quad y = -1 \quad and \quad \theta_2 = 1 \quad at \quad y = 1 \tag{31}$$

(ii) at the fluid interface temperature (θ) and heat flux ($\bar{\mathbf{h}}$) are continuous:

$$\theta_1 = \theta_2 \quad and \quad \frac{d\theta_1}{dy} = n_k\frac{d\theta_2}{dy} \quad at \quad y = 0 \tag{32}$$

The solutions of Eqs. (29) and (30) are given by

$$\begin{aligned}\theta_1(y) = Br[&P_1y^4 + P_2y^3 + P_3y^2 + P_4y(c_{14}Cosh\alpha_1y \\ &+ c_{13}Sinh\alpha_1y) + P_5Cosh\alpha_1y + P_6Sinh\alpha_1y \\ &+ P_7Cosh2\alpha_1y + P_8Sinh2\alpha_1y] + c_{15}y + c_{16}\end{aligned} \tag{33}$$

$$\begin{aligned}\theta_2(y) = \frac{Br}{n_k}[&P_9y^4 + P_{10}y^3 + P_{11}y^2 + P_{12}y(c_{13}Cosh\alpha_2y \\ &+ c_{14}Sinh\alpha_2y) + P_{13}Cosh\alpha_2y + P_{14}Sinh\alpha_2y \\ &+ P_{15}Cosh2\alpha_2y + P_{16}Sinh2\alpha_2y] + c_{25}y + c_{26}\end{aligned} \tag{34}$$

The solution involves 4 constants c_{15}, c_{16}, c_{25} and c_{26} and these are found from the 4 boundary conditions ((31) and (32)) and are obtained using Mathematica. Also all P_i's (i = 1–16) are known constants involving the constants c_{11}, c_{12}, c_{13}, c_{14}, c_{21}, c_{22}, c_{23} and c_{24}.

5.4. Nusselt number

Heat transfer coefficient at the walls is given by Fourier's law $\bar{\mathbf{h}} = -k\nabla T$. In non-dimensional form this represents Nusselt number $Nu = -\frac{d\theta}{dy}\Big]_{y=\pm1}$. This is studied only at the walls of the channel.

6. Entropy generation

6.1. The volumetric entropy generation

It is assumed that each micropolar fluid of the constant physical properties (ρ, μ, k, c_p) is flowing in the channel subjected to constant wall temperatures on the each plate. If we take an infinitesimal fluid element in each zone and assume that the element as an open thermodynamic system subjected to mass fluxes, energy transfer and entropy transfer interactions through a fixed control surface. The volumetric rate of entropy generation for incompressible micropolar fluid is given as

$$\begin{aligned}(S_i)_G = &\frac{k_i}{T_o^2}\left(\frac{\partial T_i}{\partial Y}\right)^2 + \frac{\mu_i}{T_o}\left(\frac{\partial U_i}{\partial Y}\right)^2 + \frac{\kappa_i}{T_o}\left(\frac{\partial U_i}{\partial Y} + 2C_i(Y)\right)^2 \\ &+ \frac{\beta_i}{T_o}\left(\frac{\partial C_i}{\partial Y}\right)^2\end{aligned} \tag{35}$$

where the value of i can be either 1 or 2 that represent fluid I and fluid II, respectively. The right hand side of the above equation the first term represents the heat conduction and the remaining three terms represent the viscous dissipation function, Φ for an incompressible micropolar fluid.

6.2. The characteristic entropy generation rate

The dimensionless entropy generation number Ns [1] is obtained by dividing the total entropy transfer rate $(S_i)_G$ (in Eq. (35)) with the characteristic entropy rate $(S_i)_{G,C}$ that is defined as

$$(S_i)_{G,C} = \left[\frac{(\bar{\mathbf{h}}_i)^2}{k_iT_o^2}\right] = \left[\frac{k_i(\Delta T_i)^2}{h^2T_o^2}\right] \tag{36}$$

6.3. The entropy generation number

In the above equation, $\bar{\mathbf{h}}_i$ is the heat flux, T_o is the absolute reference temperature, ΔT_i is the reference temperature (entrance temperature) difference and h is the characteristic length that depends on geometry and type of problem. Here it is equal to the half transverse distance of the channel. The entropy generation number for each fluid with dimensionless variables are given by

$$\begin{aligned}Ns_1 = &\left(\frac{d\theta_1}{dy}\right)^2 \\ &+ \frac{Br}{\Omega}\left[\left(\frac{du_1}{dy}\right)^2 + c_1\left(\frac{du_1}{dy} + 2\mathcal{C}_1\right)^2 + \delta_1\left(\frac{d\mathcal{C}_1}{dy}\right)^2\right]\end{aligned} \tag{37}$$

$$\begin{aligned}Ns_2 = &\left(\frac{d\theta_2}{dy}\right)^2 \\ &+ \frac{Br}{n_k\Omega}\left[n_\mu\left(\left(\frac{du_2}{dy}\right)^2 + c_2\left(\frac{du_2}{dy} + 2\mathcal{C}_2\right)^2\right) + \delta_1n_\beta\left(\frac{d\mathcal{C}_2}{dy}\right)^2\right]\end{aligned} \tag{38}$$

where $Br = \left(\frac{\mu_1 U_o^2}{k_1 \Delta T}\right)$ is the Brinkman number, which determines importance of viscous dissipation because of the fluid frictions relative to the conduction heat flow resulting from the impressed temperature difference and $\Omega = \left(\frac{\Delta T}{T_o}\right)$ is the dimensionless temperature difference.

In order to obtain a global Brinkman number that is valid for the both fluids confined in the channel, in the above equations the characteristic entropy transfer rates of the fluids are taken to be equal to one another as follows:

$$(S_1)_{G,C} = (S_2)_{G,C} = \left(\frac{\bar{\mathbf{h}}_1^2}{k_1 T_o^2}\right) = \left(\frac{k_1 (\Delta T_1)^2}{h^2 T_o^2}\right)$$

Eqs. (37), (38) can be expressed alternatively as follows:

$$Ns_i = Ny_i + Nf_i \tag{39}$$

On the right hand side of Eq. (39) the first term (Ny_i) denotes the entropy generation by heat transfer due to transverse conduction, the second term (Nf_i) represents the entropy generation due to viscous dissipation effect that results from the fluid frictions. The entropy generation number for both the fluids in terms of dimensionless temperature distributions are given by Eqs. (37) and (38).

It is desirable to consider the *Ek* and *Pr* in a group that is called the Brinkman number ($Br = Ek.Pr$) for evaluating the relative importance of the energy due to viscous dissipation to the energy because of heat conduction. It was reported that Br is much less than unity for many engineering processes [1]. The irreversibility distribution ratio ϕ is defined as the ratio of entropy generation due to fluid frictions (Nf) to heat transfer in transverse direction (Ny) i.e., $\phi = \left(\frac{Nf}{Ny}\right)$. The viscous dissipation parameter is an important dimensionless number for the irreversibility analysis. It determines the relative importance of the viscous effects for the entropy generation and it is equal to the ratio of Brinkman number to the dimensionless temperature difference i.e.,$\left(\frac{Br}{\Omega}\right)$. The irreversibility distribution ratio ϕ can be interpreted as follows:If $0 \leqslant \phi < 1$, then ϕ indicates that heat transfer irreversibility dominates and if $\phi > 1$ the fluid friction dominates. For the case of $\phi = 1$, both the heat transfer and fluid friction have the same contribution for entropy generation.

6.4. The Bejan number

An alternative irreversibility distribution parameter was defined by Paoletti et al. [43] as ratio of entropy generation due to heat transfer to the total entropy generation that is called Bejan number given by

$$Be = \frac{Ny}{Ns} = \frac{Ny}{Ny + Nf} = \frac{1}{1+\phi} \tag{40}$$

The above equation can be interpreted according to values of ϕ as described above. Hence, the range of Bejan number is between 0 and 1. The value of $Be \to 1$ indicates that the heat transfer irreversibility dominates over fluid friction, which corresponds to the case of $\phi \to 0$. On the other hand, if $Be \to 0$ indicates that the fluid friction irreversibility dominates over the irreversibility due to the heat transfer, which corresponds the limit of $\phi \to \infty$. The case of $Be = \frac{1}{2}$ shows that the entropy generation due to heat transfer and fluid friction irreversibility are of same order, and corresponds to the case of $\phi = 1$. By substituting Eqs. (37) and (38) into Eq. (40) with considering Eq. (39), Bejan number, in terms of dimensionless temperature, can be obtained as follows for each fluid.

$$Be_1 = \frac{Ny_1}{Ns_1}, Be_2 = \frac{Ny_2}{Ns_2} \tag{41}$$

6.5. Importance of second law

By first law of thermodynamics, we can find the temperature distributions of fluids within the channel and heat transfer coefficients can be calculated at the walls. But this law will not give the information regarding relative effects of viscosity and heat convection for entropy generation. Second law states that entropy is always positive and the law is stated in the form of inequality of entropy generation. Second law analysis makes it possible to compare many different interactions in a system, and to identify the major sources of exergy destructions/losses. Hence within the entire fluid region where exactly the entropy generation is more, can be studied by second law. To study this effect Bejan [1,2] introduced entropy generation number (Ns). Relative effects of dissipation energy and heat transfer can be studied by Bejan number (Be) [43].

7. Results and discussion

Exact solutions for the flow of two immiscible micropolar fluids are obtained and reported in the previous section. These solutions are evaluated numerically and depicted graphically. The variations of velocity, micro-rotation, temperature and entropy generation rate for different values of parameters are shown through figures.

7.1. Effect of couple stress parameter (s_i)

From Figs. 2–6 we notice that as couple stress parameter s_2 increases, velocity, micro-rotation, temperature and entropy generation number are increasing. As $s_2 \to \infty$ we get the case of Newtonian (viscous) fluids. Hence Fig. 2 indicates that the velocities of viscous fluids is more than the velocities of the micropolar fluids. But the velocities will change slightly by increasing s_2. A part of velocity in micropolar fluids is due to couple stress tensor generated by rotation of particles. Hence we conclude that in one dimensional straight flow, the effect of couple stresses on velocity is small. From Fig. 3, we see that the effect of couple stresses on micro-rotation is very high. Hence we can say that couple stresses can effect micro-rotation very much and velocity slightly. Since velocity is changing slightly, the temperature due to dissipation of energy (depending on velocity) also changes very slightly. This is seen in Fig. 4, as s_2 increases temperature increases slightly. The same effect is seen on entropy generation number Ns in Fig. 5. But near the plates effect of couple stresses on Ns is considerable.

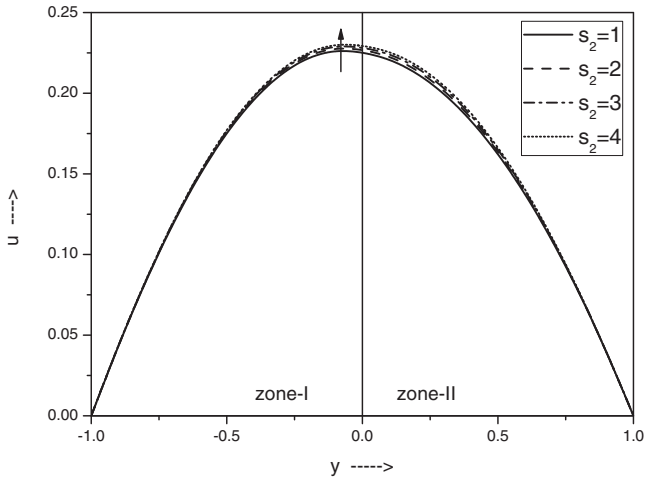

Fig. 2. Effect of couple stress parameter s_2 on velocity u for $B = -0.8$, $c_1 = 0.1$, $c_2 = 1.2$, $Re = 1.2$, $n_\rho = 0.6$, $n_\beta = 0.9$, $n_\mu = 0.6$, $s_1 = 2$.

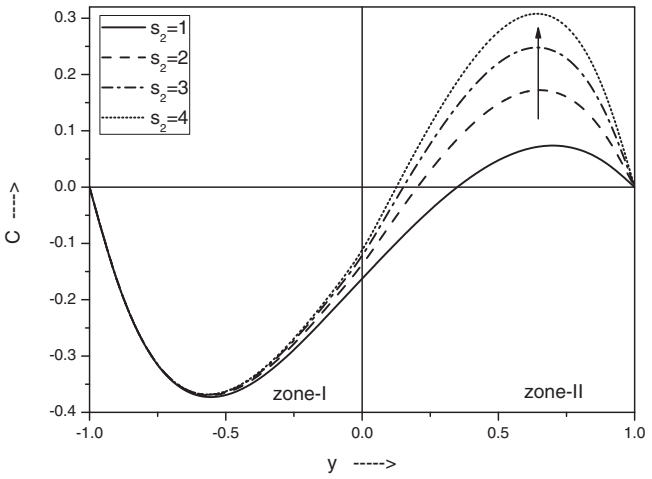

Fig. 3. Effect of couple stress parameter s_2 on microrotation $\mathcal{C}$ for $B = -2$, $c_1 = 3$, $c_2 = 3$, $Re = 3$, $n_\rho = 0.6$, $n_\beta = 0.8$, $n_\mu = 0.5$, $s_1 = 5$.

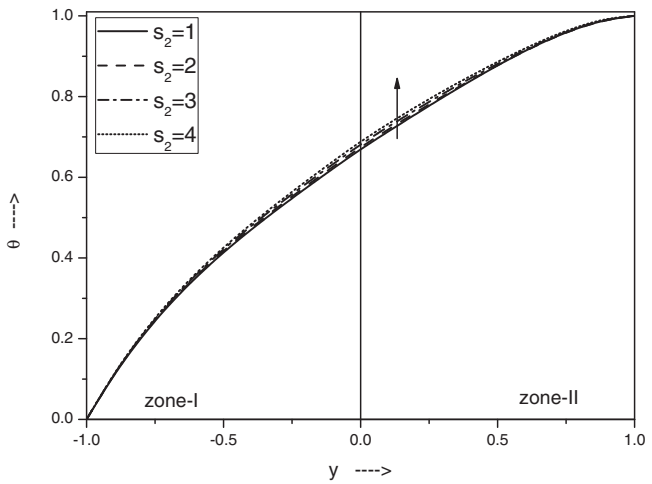

Fig. 4. Effect of couple stress parameter s_2 on temperature θ for $B = -1$, $Br = 2$, $c_1 = 0.8$, $c_2 = 1.2$, $n_k = 1.1$, $n_\rho = 0.6$, $n_\mu = 0.3$, $n_\beta = 0.9$, $\delta_1 = 0.7$, $Re = 2$, $s_1 = 2$.

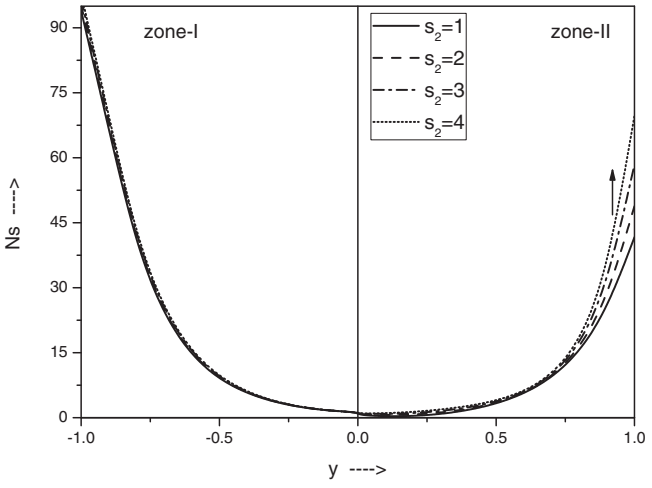

Fig. 5. Effect of couple stress parameter s_2 on entropy generation number Ns as a function of y for $B = -2$, $Br = 0.4$, $c_1 = 0.11$, $c_2 = 0.11$, $n_\mu = 0.8$, $n_\rho = 0.8$, $\delta_1 = 0.8$, $n_\beta = 0.9$, $n_k = 1.1$, $R = 2$, $s_1 = 6$, $\Omega = 1$.

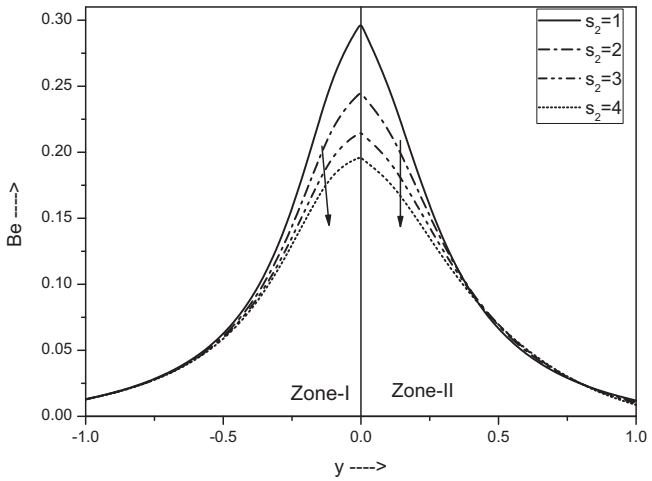

Fig. 6. Effect of couple stress parameter s_2 on Bejan number Be as a function of y for $B = -1.2$, $Br = 0.5$, $c_1 = 1.5$, $c_2 = 1.5$, $n_\mu = 0.8$, $n_\rho = 0.6$, $\delta_1 = 0.6$, $n_\beta = 0.9$, $n_k = 1.5$, $R = 4$, $s_1 = 2$, $\Omega = 1$.

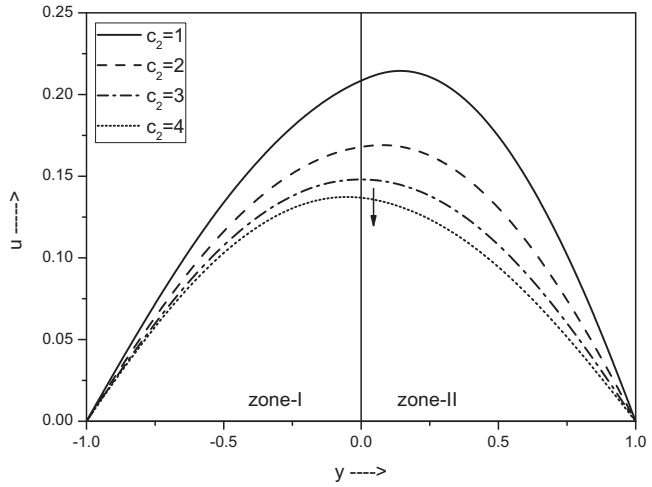

Fig. 7. Effect of micropolarity parameter c_2 on velocity u for $B = -0.5$, $c_1 = 2$, $Re = 1.5$, $n_\rho = 0.7$, $n_\beta = 0.8$, $n_\mu = 0.5$, $s_1 = 5$, $s_2 = 5$.

This may be due to more friction near the walls. From Fig. 6 we see that Bejan number is high at the interface. From the limiting case of $s_2 \to \infty$, we see that Be for viscous fluids is less than the micropolar fluids. A slight increase in couple stress parameter s_2, increases Bejan number Be very much at the interface. Since Be is nearly zero near to the plates, entropy generation rate in transverse direction is almost zero and fluid friction dominates.

7.2. Effect of cross viscosity or micro-polarity parameter (c_i)

From Figs. 7–11. We observe that as micropolarity parameter c_2 increases, velocity decreases considerably, micro-rotation decreases numerically and temperature decreases. But Bejan number Be increases. As $c_2 \to \infty$, fluid particles will rotate about themselves with high angular velocities and hence fluid velocity decreases, as most of the momentum of the particles is transferred to the rotation of the particles. Since velocity is decreasing, dissipation of energy due to velocity decreases and hence temperature decreases. In Fig. 10, the variation of the entropy generation number Ns is shown, which varies in entire region of y with variation in c_2 is shown. We observe that Ns is minimum at interface and

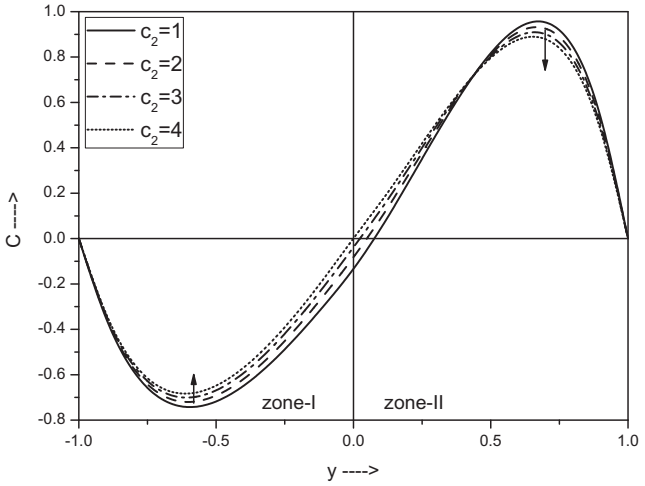

Fig. 8. Effect of micropolarity parameter c_2 on microrotation C for $B = -3$, $c_1 = 1.2$, $Re = 1.5$, $n_\rho = 0.6$, $n_\beta = 0.8$, $n_\mu = 0.4$, $s_1 = 5$, $s_2 = 8$.

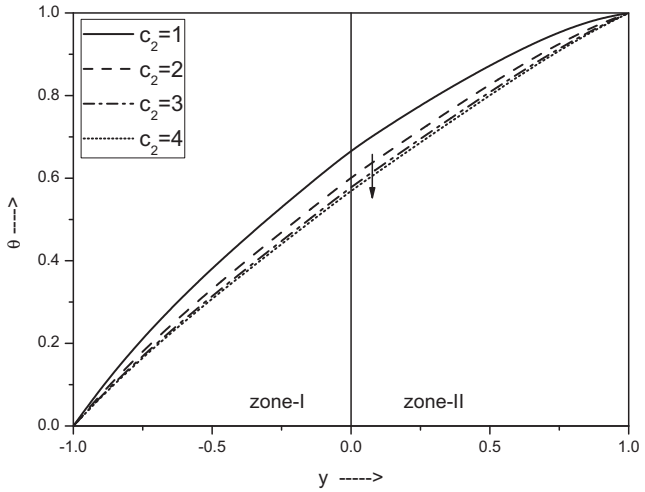

Fig. 9. Effect of micropolarity parameter c_2 on temperature θ for $B = -1.3$, $Br = 0.6$, $c_1 = 1.3$, $n_k = 1.1$, $n_\mu = 0.4$, $n_\rho = 0.9$, $n_\beta = 0.9$, $\delta_1 = 0.7$, $Re = 2$, $s_1 = 2$, $s_2 = 2$.

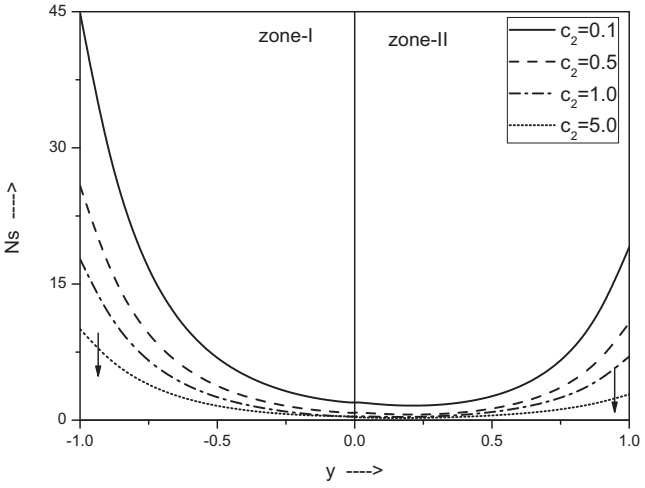

Fig. 10. Effect of micropolarity parameter c_2 on entropy generation number Ns as a function of y for $B = -2.5$, $Br = 0.8$, $c_1 = 2.5$, $n_\mu = 0.5$, $n_\rho = 0.6$, $\delta_1 = 0.6$, $n_\beta = 0.9$, $n_k = 1.1$, $R = 2$, $s_1 = 2$, $s_2 = 2$, $\Omega = 1$.

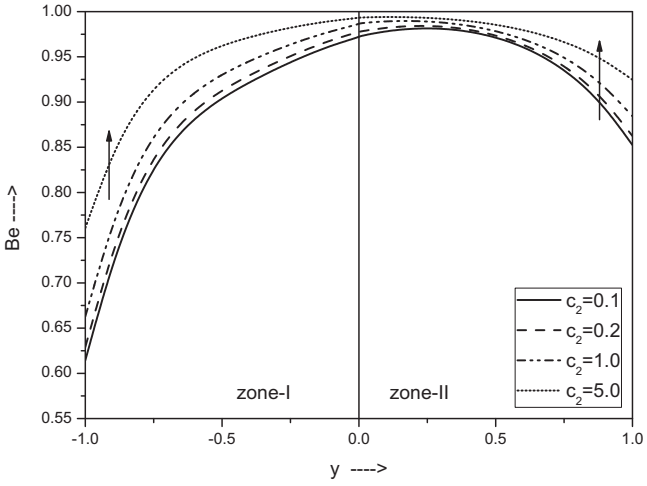

Fig. 11. Effect of micropolarity parameter c_2 on Bejan number Be as a function of y for $B = -0.1$, $Br = 0.8$, $c_1 = 2.2$, $n_\mu = 0.6$, $n_\rho = 0.6$, $\delta_1 = 0.6$, $n_\beta = 0.9$, $n_k = 1.5$, $R = 5$, $s_1 = 8$, $s_2 = 2.5$, $\Omega = 1$.

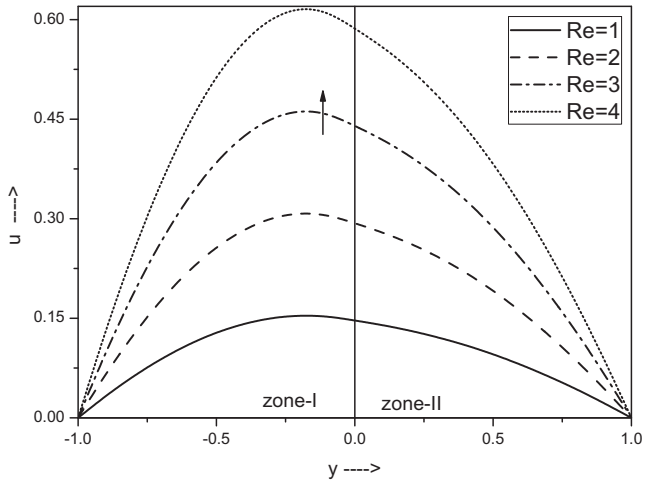

Fig. 12. Effect of Reynolds number Re on velocity u for $B = -0.8$, $c_1 = 1.2$, $c_2 = 1.5$, $n_\mu = 0.5$, $n_\rho = 0.4$, $n_\beta = 0.5$, $s_1 = 2$, $s_2 = 2$.

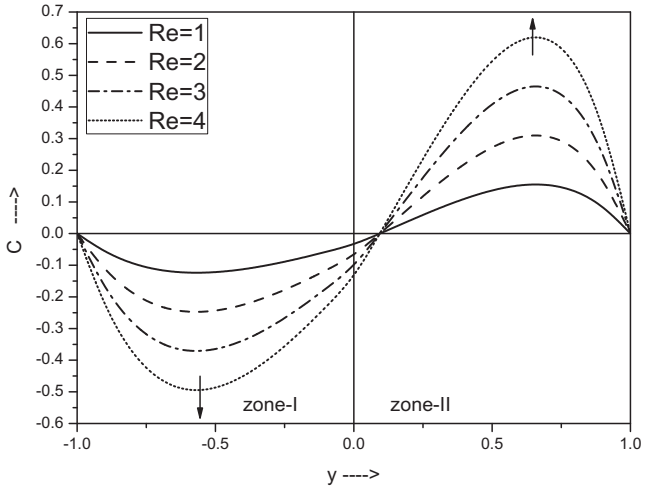

Fig. 13. Effect of Reynolds number Re on micro-rotation C for $B = -2$, $c_1 = 3$, $c_2 = 0.2$, $n_\mu = 0.5$, $n_\rho = 0.6$, $n_\beta = 0.8$, $s_1 = 5$, $s_2 = 8$

variation in c_2 will not effect *Ns* but c_2 effects *Ns* very much near the plates. The opposite behavior is seen in the case of Bejan number *Be* (Fig. 11). As c_2 increases, *Be* also increases. This is in contrast to the behavior of *Ns* as s_2 increases. We see that *Be* at any point y is more than 0.625 near the plates. This indicates that even near to the plates effect of friction is less. This is very useful property. We can conclude that micropolarity of fluids reduces the frictional effects near the walls.

7.3. Effect of Reynolds number (Re)

From Figs. 12–16 we observe that as Reynolds number *Re* increases, increasing nature in velocity, micro-rotation (numerically), temperature and entropy generation number *Ns* is seen. All these values of u, $\mathcal{C}$, θ and *Ns* raise very much with a small raise in the *Re* values. But near the walls Bejan number decreases as *Re* increases which shows high dissipation of energy or entropy generation rate near the plates. Fig. 17 shows that as Reynolds number *Re* increases, Nusselt number *Nu* increases. This may be due to rapid increase of velocity as *Re* increases.

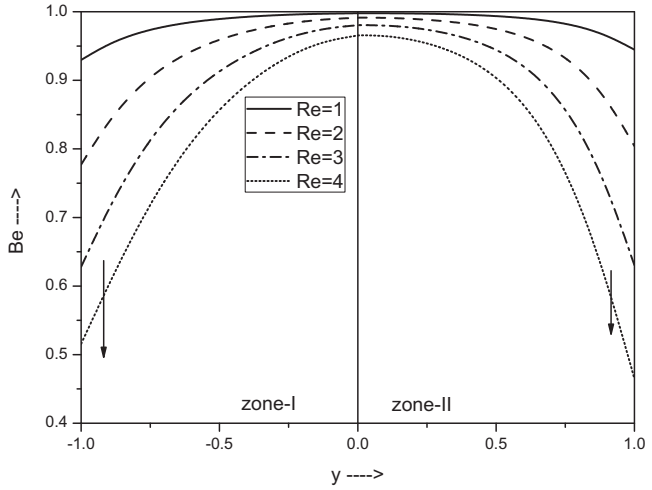

Fig. 16. Effect of Reynolds number *Re* on Bejan number *Be* as a function of *y* for $B = -0.8$, $Br = 0.1$, $c_1 = 3$, $c_2 = 3$, $n_\mu = 0.5$, $n_\rho = 0.6$, $\delta_1 = 0.6$, $n_\beta = 0.9$, $n_k = 1.1$, $s_1 = 5$, $s_2 = 5$, $\Omega = 1$.

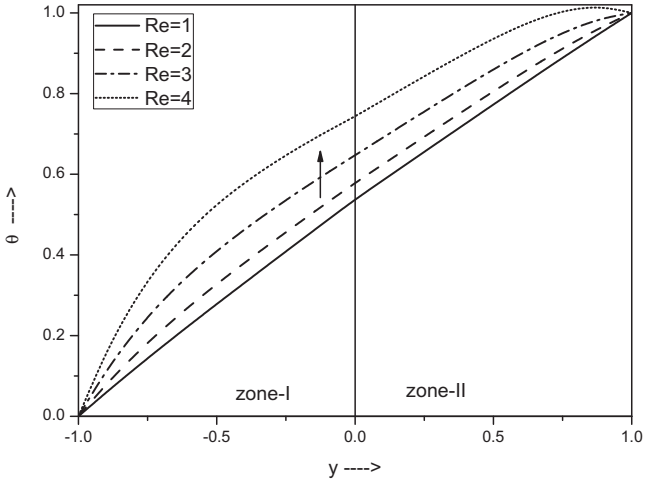

Fig. 14. Effect of Reynolds number *Re* on temperature θ for $B = -0.8$, $c_1 = 1.5$, $c_2 = 1.2$, $n_k = 1.1$, $n_\rho = 0.6$, $n_\mu = 0.8$, $n_\beta = 0.9$, $\delta_1 = 0.7$, $s_1 = 1.5$, $s_2 = 1.8$.

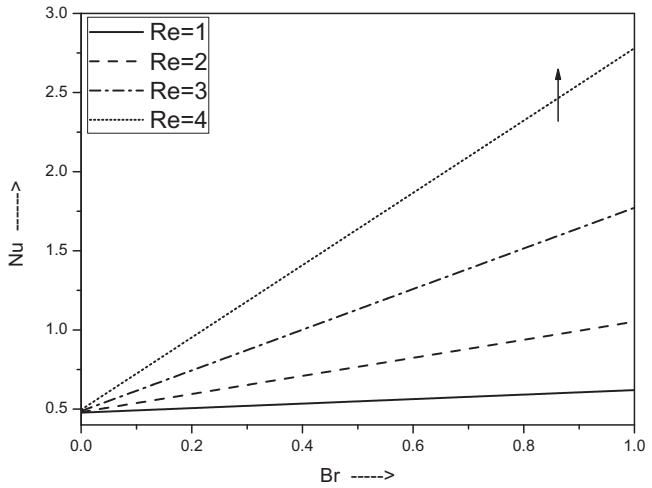

Fig. 17. Effect of Reynolds number *Re* on Nusselt number *Nu* as a function of *Br* for $B = -0.8$, $c_1 = 1.2$, $c_2 = 1.1$, $n_\mu = 0.6$, $n_\rho = 0.6$, $\delta_1 = 0.7$, $n_\beta = 0.9$, $n_k = 1.1$, $s_1 = 1.2$, $s_2 = 1.2$.

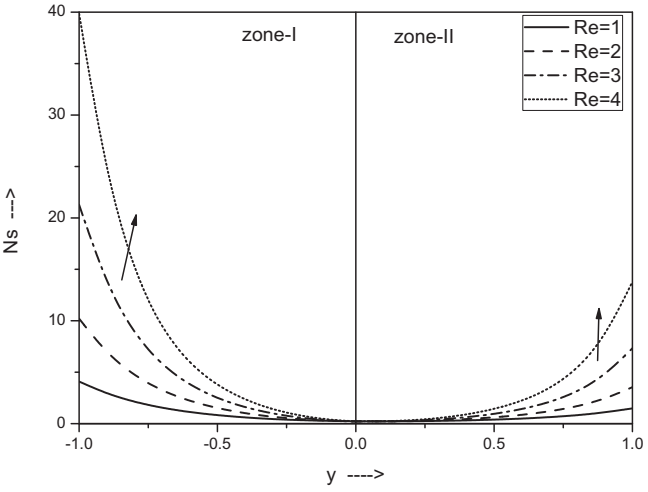

Fig. 15. Effect of Reynolds number *Re* on Entropy generation number *Ns* as a function of *y* for $B = -2$, $Br = 0.5$, $c_1 = 2.5$, $c_2 = 3$, $n_\mu = 0.4$, $n_\rho = 0.6$, $\delta_1 = 0.6$, $n_\beta = 0.9$, $n_k = 1.1$, $s_1 = 2$, $s_2 = 2$, $\Omega = 1$.

7.4. Effect of viscous dissipation parameter $\left(\frac{Br}{\Omega}\right)$

Dissipation parameter $\frac{Br}{\Omega}$ occurs only in the equations for temperatures. The effect of the parameter $\frac{Br}{\Omega}$ on entropy generation number *Ns* and on Bejan number *Be* is shown in Figs. 18 and 19. A small raise in the values of $\frac{Br}{\Omega}$, increases the values of entropy generation number *Ns* and decreases the values of Bejan number *Be* very much. The figures indicate that at the interface $y = 0$, entropy generation rate is minimum i.e., available energy in transverse direction at the interface is maximum. At the walls *Be* is minimum and *Ns* is maximum i.e., the fluid friction dominates near the walls. These results are similar to the results obtained by Subba Reddy et al. [44].

From Figs. 6 and 11, the comparative study of effect of couple stress parameter s_2 and micropolarity parameter c_2 on *Be* shows that near the walls s_2 has no effect but c_2 increases the values of *Be*. Again we observed that *Be* is more than 0.625 near the walls for c_2 and *Be* is almost zero near the walls for s_2 in Figs. 6 and 11. This indicates that micropolarity parameter offers smoothness to the walls and hence friction near the walls deceases. This shows

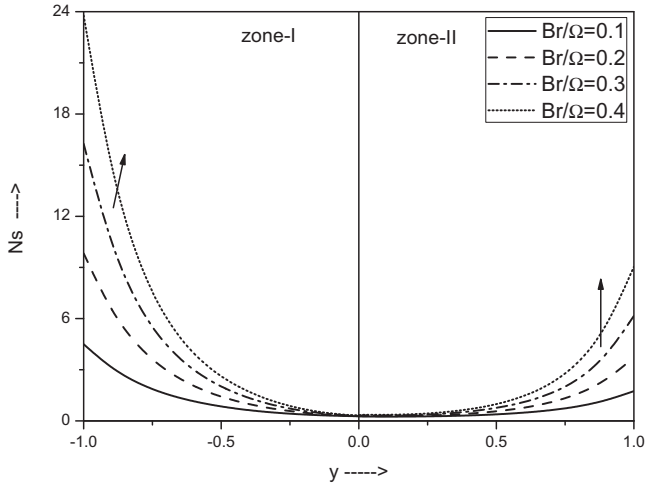

Fig. 18. Effect of viscous dissipation parameter $\frac{Br}{\Omega}$ on Entropy generation number *Ns* as a function of *y* for $B = -3$, $c_1 = 2.5$, $c_2 = 3$, $n_k = 1.1$, $n_\rho = 0.6$, $n_\mu = 0.4$, $n_\beta = 0.9$, $\delta_1 = 0.6$, $Re = 3$, $s_1 = 5$, $s_2 = 5$, $\Omega = 1$.

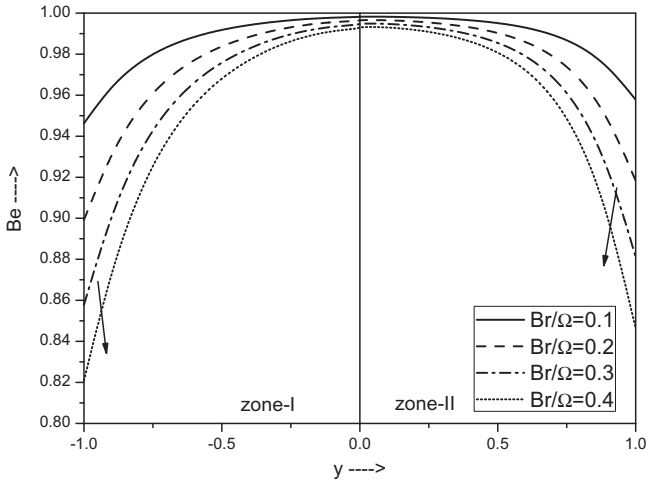

Fig. 19. Effect of viscous dissipation parameter $\frac{Br}{\Omega}$ on Bejan number *Be* as a function of *y* for $B = -0.8$, $c_1 = 2.5$, $c_2 = 2.5$, $n_k = 1.1$, $n_\rho = 0.6$, $n_\mu = 0.5$, $n_\beta = 0.6$, $Re = 0.8$, $s_1 = 5$, $s_2 = 5$, $\Omega = 1$.

an industrial application that micropolar fluids with high micropolarity and less couples stresses will act as a good lubricant. The reason for this may be due to the fact that much of momentum of the fluid particles is transferred to the rotation of the particles by decreasing their velocity. Hence friction and dissipation of energy decreases near the plates.

7.5. Effect of ratio of viscosities (n_μ)

In Fig. 20, we observe that as $n_\mu\left(=\frac{\mu_2}{\mu_1}\right)$ increases, velocity decreases. This may be due to the fact that as n_μ increases, viscosity increases and offers more resistance to flow. Hence velocity decreases.

The similar results are observed by Umavathi et al. [33] in the flow of viscous fluids in horizontal channel and by Prathap Kumar et al. [34] in the flow of micropolar and viscous fluids in vertical channel.

As a special case of micropolar fluids (as $c \to 0$, $s \to \infty$, we get viscous fluids) our results are in agreement with the observations of [33,34].

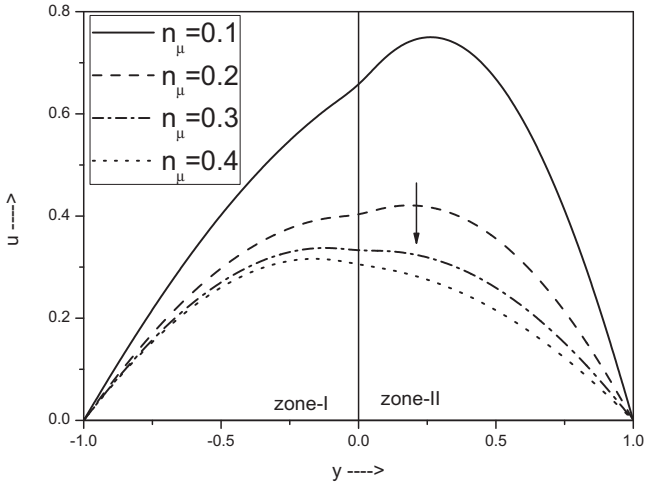

Fig. 20. Effect of ratio of viscosity on velocity for $B = -0.8$, $c_1 = 1.2$, $c_2 = 1.5$, $n_\rho = 0.4$, $n_\beta = 0.5$, $Re = 2.0$, $s_1 = 2.0$, $s_2 = 2.0$.

8. Conclusion

The flow of immiscible micropolar fluids between two parallel plates due to the constant pressure gradient is studied. The velocity, micro-rotation and temperature distributions are found analytically. The exergy loss distribution is studied in terms of second law of thermodynamics. The entropy generation number *Ns* at every point y between the channels is found. The effect of viscous dissipation parameter $\frac{Br}{\Omega}$ on entropy generation number (*Ns*), Bejan number (*Be*) is studied through figures.

It is observed that:

1. Near the plates the values of *Ns* are more than the values of *Ns* at the interface, indicating that friction due to surfaces on the fluids increases entropy generation rate.
2. Near the plates in zone-I values of *Ns* are more than the values of *Ns* in zone-II. This indicates the more the viscosity of the fluid is, the more the entropy generation.
3. At the interface of the fluids Bejan number is maximum and hence irreversibility ratio ϕ is minimum. This indicates that amount of exergy (available energy) is maximum and irreversibility is minimum at the interface between the fluids.
4. Based on limiting values of micropolarity parameter and couple stress parameter, we conclude that the values of velocity, temperature and entropy generation number for viscous fluid are more than the corresponding values for micropolar fluid case. This may be due to the fact that in viscous fluids microrotations are absent and hence exergy is not used for this purpose.
5. As micropolarity increases, entropy generation number at the plates decreases and Bejan number increases. This indicates an industrial application for micropolar fluids to use them as a good lubricant.

Acknowledgements

The authors thank the reviewers for their constructive comments for the improvement of the paper to a great extent.

References

[1] Adrian Bejan, A study of entropy generation in fundamental convective heat transfer, J. Heat Transfer 101 (1979) 718–725.
[2] Adrian Bejan, Second law analysis in heat transfer, Energy 5 (1980) 721–732.

[3] Adrian Bejan, Fundamentals of exergy analysis, entropy generation minization and generation of flow architecture, Int. J. Energy Res. 26 (2002) 545–565.
[4] Adrian Bejan, Entropy Generation Minimization, CRC Press, Boca Raton, NY, 1996.
[5] Adrian Bejan, Second-law analysis in heat transfer and thermal design, Adv. Heat Transfer 15 (1982) 1–58.
[6] Adrian Bejan, Advanced Engineering Thermodynamics, John Wiley and Sons, 2006.
[7] Adrian Bejan, Convection Heat Transfer, John Wiley and Sons, 2004.
[8] Adrian Bejan, G. Tsatsaronis, M. Moran, Thermal Design and Optimization, Wiley, New York, 1996.
[9] Sayavur I. Bakhtiyarov, Dennis A. Siginer, A note on the laminar core-annular flow of two immiscible fluids in a horizontal tube, in: Proceed. Int. Symposium on Liquid–Liquid Two Phase Flow and Transport Phenomena, Begell house, Inc., Santa Barbara, 1997, pp. 107–111.
[10] Ali J. Chamkha, Oscillatory flow and heat transfer in two immiscible viscous fluids, Int. J. Fluid Mech. Res. Oscill. Flow Heat Transfer Two Immiscible Viscous Fluids 31 (2004) 13–36.
[11] Fethi Kamisli, Hakan F. Oztop, Second law analysis of the 2D laminar flow of two-immiscible, incompressible viscous fluids in a channel, Heat Mass Transfer 44 (2008) 751–761.
[12] Shohel Mahmud, Roydon Andrew Fraser, Flow, thermal, and entropy generation characteristics inside a porous channel with viscous dissipation, Int. J. Therm. Sci. 44 (2005) 21–32.
[13] A.Z. Sahin, Irreversiblities in various duct geometries with constant wall heat flux and laminar flow, Exergy 23 (1998) 465–473.
[14] A.Z. Sahin, Second law analysis of laminar viscous flow through a duct subject to constant wall temperatures, J. Heat Transfer 120 (1998) 76–83.
[15] A.X. Sahin, A second law comparison for optimum shape of subjected to constant wall temperature and laminar flow, Heat Mass Transfer 33 (1998) 425–430.
[16] Hakan F. Oztop, Effective parameters on second law analysis for semicircular ducts in laminar flow and constant wall heat flux, Int. Commun. Heat Mass Transfer 32 (2005) 266–274.
[17] A.C. Eringen, The theory of micropolar fluids, J. Math. Mech 16 (1966) 1–18.
[18] A.C. Eringen, Microcontinnum Field Theories. II: Fluent Media, Springer, New York, 2001.
[19] N.P. Migun, Experimental method of determining parameters characterizing the microstructure of micropolar fluids, J. Eng. Phys. Thermophys. 41 (1981) 832–835 (Translated from Inzhenerno-Fizicheskii Zhurnal, vol. 41, 1983, pp 220–224).
[20] V. Kolpashchikov, N.P. Migun, P.P. Prokhorenko, Experimental determination of material micropolar fluid constants, J. Eng. Sci. 21 (1983) 405–411.
[21] V.K. Stokes, Theories of Fluids with Microstructures, Springer, New York, 1984.
[22] Teoman Ariman, Ahmet S. Cakmak, Some basic viscous flows in micropolar fluids, Rheol. Acta 7 (1968) 236–242.
[23] G. Lukaszewicz, Micropolar Fluids: Theory and Applications, Birkhauser, Boston, 1999.
[24] Jerome Delhommelle, Denis J. Evans, Poiseuille flow of a micropolar fluid, Mol. Phys. Int. J. Interface Chem. Phys. 100 (2002) 2857–2865.
[25] P. Chaturani, R. Ponnalagar Samay, A study of non-Newtonian aspects of blood flow through stenosed arteries and its applications in arterial diseases, J. Biol. (1985).
[26] R.B. Bird, W.E. Stewart, E.N. Lightfoot, Transport Phenomena, John Wiley and Sons, Inc., New York, 1960.
[27] J.N. Kapur, J.B. Shukla, The flow of incompressible immiscible fluids between two parallel plates, Appl. Sci. 13 (1962).
[28] R.N. Bhattacharya, The flow of immiscible fluids between rigid plates with a time dependent pressure gradient, Bull. Calcutta Math. Soc. 1 (1968) 129–137.
[29] H. Hikita, K. Ishimi, Mass transfer into a laminor fluid stream from the moving interface of two immiscible fluids between parallel plates, Chem. Eng. J. (1977) 179–183.
[30] Jie Li, Yuriko Renardy, Numerical study of flows of two immiscible liquids at low Reynolds number, SIAM 42 (2000) 417–439.
[31] Ali J. Chamkha, Flow of two immiscible fluids in porous and nonporous channels, J. Fluids Eng. 121 (2000) 117–124.
[32] M.S. Malashetty, J.C. Umavathi, J. Prathap Kumar, Convective magnetohydrodynamic two fluid flow and heat transfer in an inclined channel, Heat Mass Transfer 37 (2001) 259–264.
[33] J.C. Umavathi, Ali J. Chamkha, Abdul Mateen, Ali Al-Mudhaf, Unsteady two-fluid flow and heat transfer in a horizontal channel, Heat Mass Transfer 42 (2005) 81–90.
[34] J. Prathap Kumar, J.C. Umavathi, Ali J. Chamkha, Ioan Pop, Fully-developed free-convective flow of micropolar and viscous fluids in a vertical channel, Appl. Math. Model. 34 (2010) 1175–1186.
[35] D. Nikodijevic, Z. Stamenkovic, D. Milenkovic, MHD Couette two-fluid flow and heat transfer in presence of uniform inclined magnetic field, Heat Mass Transfer (2011) 1525–1535.
[36] D. Nikodijevic, Z. Stamenkovic, D. Milenkovic, B. Blagojevic, J. Nikodijevic, Flow and Heat Transfer of Two Immiscible Fluids in the Presence of Uniform Inclined Magnetic Field, Hindawi Publishing Corporation, 2011.
[37] A.Z. Szeri, K.R. Rajagopal, Flow of a non-Newtonian fluid between heated parallel plates, Int. J. Non-Linear Mech. 20 (2) (1985) 91–101.
[38] D.A. Nield, A.V. Kuznetsov, Ming Xiong, Thermally developing forced convection in a porous medium: parallel plate channel with walls at uniform temperature, with axial conduction and viscous dissipation effects, Int. J. Heat Mass Transfer (2003) 643–651.
[39] S.K. Jena, M.N. Mathur, Similarity solutions for laminar free convection flow of a thermo-micropolar fluid past a non-isothermal vertical flat plate, Int. J. Eng. Sci 19 (1981) 1431–1439.
[40] J. Peddieson, An application of the micropolar fluid model to the calculation of turbulent shear flow, Int. J. Eng. Sci 10 (1972) 23–32.
[41] D.A.S. Rees, Andrew P. Bossom, The Blasius boundary layer flow of a micropolar fluid, Int. J. Eng. Sci. 34 (1996) 113–124.
[42] K. Bhattacharyya, S. Mukhopadhyay, Layek G. C, Ioan Pop, Effects of thermal radiation on micropolar fluid flow and heat transfer over a porous shrinking sheet, Int. J. Heat Mass Transfer 55 (2012) 2945–2952.
[43] S. Paoletti, F. Rispoli, E. Sciubba, Calculation exergetic loses in compact heat exchanger passages, ASME AES 10 (1989) 21–29.
[44] R.S.R. Gorla, Second law analysis of mixed convection in a laminar, non-Newtonian fluid flow through a vertical channel, Int. Schol. Res. Netw. Appl. Math. (2011) 1–13 (Article ID 287691).